

Antiproliferative activity, apoptotic induction, cell cycle arrest and p53 expression for dual herbal combination of *W. somnifera* with three Rasayana herbs: *In vitro* cytotoxic study against Jurkat cells

Bhargavi Srinivasan^{a,*} & Madhan Shankar S R^b

^aDepartment of Biotechnology, Kongunadu Arts and Science College, Coimbatore 641 029, Tamil Nadu, India

^bAshwinis Herbs and Foods, Coimbatore 641 025, Tamil Nadu, India

*E-mail: sbhargavi_bt@kongunaducollege.ac.in

Received 01 May 2025; revised 07 February 2026; accepted 16 March 2026

The dual herbal methanolic formulations of *Withania somnifera* combined with *Phyllanthus emblica* (WP3), *Bacopa monnieri* (WB2), and *Ocimum basilicum* (WO3), prepared using our previously optimized and validated methodology for Ayurvedic phytochemical standardization, were investigated for their therapeutic relevance against leukemia. As phytotherapy emerges as a complementary strategy to reduce chemotoxicity and support long-term cancer management, evaluating rational botanical combinations is essential for advancing evidence-based integrative approaches. For the first time, this study delineates the collective anticancer effects of *W. somnifera* with three Rasayana co-herbs against Jurkat E6-1 T-cell leukemia cells. The extracts WP3 and WO3 were assayed for MTT cytotoxicity, exerting the strongest antiproliferative effects, with IC_{50} values of 20.27 and 20.40 $\mu\text{g/mL}$, respectively. We utilised Annexin V/PI flow cytometry and AO/EB staining to validate both early and late stages of apoptotic progression following treatment. The WP3 results reflected a substantial increase in apoptotic cell population for Sub-G0/G1 (18.37%) compared to (2.89%) control cells, while WO3 induced a lesser elevation of 6.53%, indicating DNA laddering resembling endonuclease fragmentation and apoptotic accumulation. Further cell cycle analysis showed reduced G0/G1 phase population for WP3 (54.79%) and WO3 (56.82%) compared to the control (69.77%), interfering with cell cycle regulatory checkpoints for DNA synthesis. p53 protein expression was upregulated in WP3 treated cells (29.52%) relative to control (9.04%), suggesting stimulation of DNA tumor suppressor signaling pathways. The dual herbal combinations, treated with WP3, showed the strongest activity, suppressing leukemic cell growth by promoting apoptotic cell death, p53-mediated responses, and altering cell cycle progression. As a first-of-its-kind study, demonstrating phytochemical profiling, preclinical validation, and initiating a framework for Rasayana-derived combinatorial therapeutic strategies.

Keywords: Apoptosis, Dual herbal combination, Jurkat cell line, p53 cell cycle, *Withania somnifera*

IPC Code: Int Cl.²⁶: A61K 36/00

The World Health Organization (WHO) indicates that Cancer continues to pose a major public health burden worldwide, with projections indicating newly diagnosed cases around 27 million by 2040, with the annual number representing an increase of approximately 50%¹. The Global Cancer Observatory (GLOBOCAN) shows a similar upward inclination in India, suggesting cancer incidence exceeding the alarming trend of 1.7 million cases by 2035. These projections together underscore growing demand for multi-target therapeutic strategies with cost-effective, favourable safety profiles, especially in low- and middle-income backgrounds where wide-ranging comprehensive cancer care remains limited².

Ayurvedic philosophy is rooted in Rasayana therapy, instating vitality, promoting nourishment, and consolidating physiological balance. Ayurvedic medicine represents traditional medicine with an extensive and largely intact source of pharmacologically relevant therapeutic choices. Rasayana, as a fundamental practice, accentuates rejuvenation, regulates the immune system, and reinforces systemic resilience against diseases. Among Rasayan-class botanicals, *Withania somnifera* (Ashwagandha), often revered as *Indian Ginseng*, has gained considerable attention for its adaptogenic and cytotoxic attributes³. Ashwagandha's roots and leaves have bioactive phytochemicals, such as withanolides, an array of alkaloids, and steroidal lactones. These phytochemicals have been reported to

*Corresponding author

trigger apoptotic pathways, suppress proliferation, and regulate oxidative stress in several cancer models. Multiple *in vitro* and *in vivo* studies consistently highlight oxidative stress across diverse cancer models. Accumulating evidence from the anticancer potential of these phytoconstituents places *W. somnifera* at the forefront of plant-based therapeutic discovery⁴⁻⁷. *Phyllanthus emblica* (Amla) possesses a diverse biochemical profile enriched with polyphenols, ellagic acid, flavonoids, and tannins, which imparts strong antioxidant, antimutagenic, and cancer-preventive properties. Experimental evidence suggests that Amla interferes with the early stages of tumour development and regulates inflammatory signalling, neutralises reactive oxygen species, and enhances DNA repair mechanisms. In addition, *Bacopa monnieri* and *Ocimum basilicum* are recognised for their neuroprotective and anti-inflammatory activities alongside growth-inhibitory effects on cancer cells. These biological actions complement the inclusivity of multi-herbal strategies, focusing on the effective efficacy of combinatorial anticancer therapies⁸⁻¹². The multi-plant therapeutic formulation contributes to a broader chemical composition interplaying with synergistic phytochemicals. Such a synergistic herbal composition contributes to the modulation of various cancer-resistance mechanisms, including programmed cell death, oxidative imbalance, and immune escape. These distinctive polyherbal formulations consistently demonstrate advantages over single-molecule drugs, achieving greater biological efficacy by harnessing contemporary modes of action while potentially reducing adverse effects and supporting pharmacological evidence.

In our previous study, antioxidant assessments defined fractional combinatorial ratios, notably WP3, WB2, and WO3, showed noticeable free radical-neutralising ability and increased bioactivity with their individual herbal counterparts. These findings served as the empirical basis for extending the investigation towards anticancer efficacy. In leukemia, T lymphocyte-mediated immune regulation is essential for sustaining immune surveillance. The T cells' oncogenic transformation disrupts immune balance, causes abnormal proliferation, defective maturation, and compromised immune competence. Jurkat E6.1 human T-lymphoblastic leukemia cell line is a standard *in vitro* model to elucidate apoptotic mechanisms, cell cycle perturbations, and therapeutic responses in T cell malignancies. The study of these

disease mechanisms using natural product-based interventions is highly relevant for proven immunomodulatory and rejuvenative activities^{13,14}.

Herbal therapeutics have been widely used to enhance immunity and modulate molecular pathways linked to cancer development. Globally, approximately 10-40% of anticancer drugs are plant-derived, increasing to approximately 50% in Asian populations dependent on traditional therapeutic remedies. Growing evidence suggests that plant-derived phytochemicals act at multiple phases of tumorigenesis by modulating apoptotic mechanisms, oxidative, and inflammatory signaling pathways^{15,16}.

In continuation of our previous work^{17,18}, dual herbal formulations of *Withania somnifera* with selected combinatorial Rasayana herbs. The dual herbal phytocombinations of WP3, WB2, and WO3 exhibited differentiating bioactive compounds, increased antioxidant activity, and distinct chemometric clustering reflecting elevated biological efficacy. Further insight into the *in silico* docking and *in vitro* experiments with these formulations demonstrated notable inhibition for SARS-CoV-2 non-structural proteins, supporting their molecular stability and multitarget pharmacological potential. Collectively, these findings indicate that defined dual combinations of *W. somnifera* and complementary Rasayana botanicals function synergistically to yield enhanced bioactivity than single plant extracts. Guided by this evidence, the present study investigates whether these optimized combinations-WP3 (*W. somnifera* + *P. emblica*), WB2 (*W. somnifera* + *B. monnieri*), and WO3 (*W. somnifera* + *O. basilicum*)- can exert anticancer effects on Jurkat E6.1 T-cell leukemia cells. Using integrated analyses of DNA fragmentation, cell-cycle control, and p53 expression, the present investigation aims to establish whether these dual formulations trigger intrinsic apoptotic signaling and interfere with major cell cycle checkpoints. Overall, this work extends our earlier standardization studies and provides mechanistic evidence supporting the anticancer efficacy of Rasayana-derived combinatorial formulations.

Materials and Methods

Chemicals

All chemicals, sera, media, and antibiotics were of analytical grade from Sigma-Aldrich, including methanol, dimethyl sulfoxide (DMSO), MTT, Roswell Park Memorial Institute 1640 media (RPMI), Streptomycin solution, agarose, and ethidium bromide

(EtBr) from Hi-Media. The standard drugs Cladribine and penicillin were sourced from Cipla, and sterile plastic materials for cell culture were obtained from Corning, USA.

Plant materials and preparation of dual combinatorial extracts

Previously, methanolic extracts of *Withania somnifera* (W) roots and their dual combinations-WP (*P. emblica* fruits), WB (*B. monnieri* leaves), and WO (*O. basilicum* leaves)-were prepared in three fractional ratios [4:1 (1), 1:1 (2), and 1:4 (3)] as detailed in our earlier study. Among these, the extracts W, WP3, WB2, and WO3 demonstrated the highest antioxidant capacity based on qualitative and quantitative HPTLC and chemometric profiling¹⁷, providing the rationale for their selection in the present work. For the subsequent *in vitro* assays, the extracts were dissolved in 0.08% DMSO, a concentration verified as non-toxic to Jurkat cells.

Jurkat E6-1 and PBMC cells

Human acute T-cell leukemia cells (Jurkat E6-1) and primary peripheral blood mononuclear cells (PBMCs, normal) were procured from the National Centre for Cell Science (NCCS), Pune. The cells were cultured in RPMI-1640 medium supplemented with 10% fetal bovine serum (FBS), 100 U/mL penicillin, and 50 µg/mL streptomycin, and maintained at 37°C in a humidified incubator with 5% CO₂ (HF240 Smart Cell, Heal Force, China)¹⁹.

Flow cytometry analysis of treated Jurkat cells

Quantification of apoptotic cells by Annexin/PI assay²⁰

Jurkat cells (0.5×10^6 cells/2 mL/well) were seeded in 6-well plates and incubated for 24 h at 37°C. Cells were treated with WP3 and WO3 (20 µg/mL) for 24 h, harvested, washed with PBS, and resuspended in Annexin-V binding buffer. Cells were stained with FITC-Annexin V (5 µL) for 15 min in the dark, followed by PI staining (4 µL in 400 µL binding buffer). A minimum of 10,000 events/sample was analyzed using a BD FACSC alibur flow cytometer (488 nm laser) and CellQuest Pro software. This dual-staining strategy differentiates early apoptotic cells (Annexin V⁺/PI⁻) from late apoptotic or necrotic cells (Annexin V⁺/PI⁺), based on phosphatidylserine externalization and membrane integrity loss²¹.

Acridine orange (AO)/Ethidium bromide (EB) fluorescent staining

AO/EB staining was used to assess apoptosis and nuclear changes. Acridine orange stains both live and

dead cells, while ethidium bromide stains only cells with compromised membrane integrity. Live cells appeared uniformly green, early apoptotic cells showed bright green nuclei with chromatin condensation, late apoptotic cells appeared orange with fragmented nuclei, and necrotic cells-stained orange but retained normal nuclear morphology. The morphological changes were examined under a fluorescence microscope with a fluoresce in filter and a 10x magnification.

Nuclear DNA fragmentation of Jurkat cells²²

DNA fragmentation was analyzed in Jurkat cells (0.5×10^6 cells/2 mL) incubated overnight at 37°C. Cells were treated with methanolic extracts of WP3 and WO3 (20 µg/mL) for 24 h, followed by PBS washing. After removing PBS, 200 µL trypsin-EDTA was added for a few minutes, and 2 mL fresh culture medium was used to harvest cells into 12 × 75 mm polystyrene tubes. Cells were centrifuged at 300 g for 5 min at 25°C, and the supernatant was discarded. Genomic DNA was isolated based on the previous study²³. A 3 µL sample from each tube was loaded onto a 2% agarose gel containing 0.1% ethidium bromide, visualized under UV light, and imaged using ImageLab software (BioRad).

The effect of the methanolic combinatorial extract on cell cycle DNA content of Jurkat cells²⁴

Jurkat cells (0.5×10^6 cells/2 mL/well) were seeded in 6-well plates and incubated for 24 h at 37°C with 5% CO₂. Cells were treated with WP3 and WO3 (20 µg/mL) for 24 h, harvested, washed with PBS, and fixed with 70% cold ethanol at -20°C. After centrifugation and PBS washing, cells were treated with RNase A and stained with Propidium Iodide (PI, 400 µL). Cell cycle distribution (Sub-G0/G1, G0/G1, S, G2/M) was analyzed by flow cytometry (BD FACSC alibur; 488 nm excitation), acquiring 20,000 events per sample. Histogram analysis was performed using CellQuest Pro (v6.0).

p53 protein analysis on Jurkat cells treated with methanolic combinatorial extracts²⁵

Jurkat cells (0.5×10^6 cells/well) were seeded in 6-well plates and incubated overnight. Cells were then treated with WP3 and WO3 (20 µg/mL) for 24 h. After treatment, cells were collected, washed with PBS, and fixed in 70% chilled ethanol for 30 min on ice. Following centrifugation, cells were permeabilised using BD Cytotfix/Cytoperm for 10 min and washed with 0.5% BSA in PBS containing 0.1% sodium azide. Subsequently, cells were incubated

with 20 μL FITC-conjugated mouse anti-p53 antibody for 30 min in the dark at room temperature. Following a final wash with PBS, quantified using flow cytometric analysis with fluorescence detection at an excitation/emission wavelength of 650 nm.

Statistical Analysis

All experiments were performed in triplicate ($n = 3$) and repeated at least three times to ensure reproducibility. Data values are denoted as mean \pm standard deviation (SD).

Results and Discussion

In vitro Jurkat E6-1 anticancerous activity

Based on our MTT assay outcomes, only the most relevant findings that guided the subsequent apoptosis investigations are briefly summarized here. Among the tested formulations, the dual-herbal combinations *Withania somnifera-Phyllanthus emblica* (WP3) and *Withania somnifera-Ocimum basilicum* (WO3) exhibited markedly enhanced antiproliferative activity against Jurkat E6-1 leukemia cells, with IC_{50} values of 20.27 and 20.40 $\mu\text{g}/\text{mL}$, respectively. The polyherbal combinations of WB2 (53.10 $\mu\text{g}/\text{mL}$) and W alone (69.40 $\mu\text{g}/\text{mL}$) were remarkably higher compared to the former, suggesting synergistic interactions. The cell viability for both Jurkat treated cells with WP3 and WO3, around 25 $\mu\text{g}/\text{mL}$ had a marked reduction in the viability ($\approx 42\text{-}48\%$), compared with the positive control, cladribine. The minimal cytotoxicity

of both WP3 and WO3 for normal PBMCs (IC_{50} : 129.6 and 108.65 $\mu\text{g}/\text{mL}$) demonstrated preferential toxicity towards leukemia cells. The statistical analysis was tested with One-way ANOVA with Tukey's post-hoc ($p < 0.05$ – $p < 0.0001$), and the results were significant for the treatment. In view of their improved selectivity and cytotoxic potency, WP3 and WO3 were further selected for subsequent apoptosis targeting pathways (Supplementary Fig. S1).

Apoptosis: FACS analysis

Flow cytometric analysis using Annexin V-FITC/PI has shown a dose-dependent apoptotic induction by the WP3 and WO3 extracts. Both the extracts WP3 and WO3 (20 $\mu\text{g}/\text{mL}$) were selected, and WB2 was excluded based on the MTT assay results. As apoptosis is a regulated form of cell death, it does not elicit inflammatory necrosis, but represents a key mechanism for effective anticancer therapy²⁶. The proapoptotic morphological alterations, like membrane blebbing, nuclear shrinkage, nuclear condensation, and DNA fragmentation, were exhibited by the WP3 and WO3-treated Jurkat cells, confirming their apoptotic potential²⁷. Flow cytometric analysis (Fig. 1a-c), revealed 18.33% early apoptotic cells treated with WP3 and 4.26% for WO3, while untreated control cells had largely viable population of 99.97%. The observed transition of cells from the M1 (Annexin V-negative) to M2 (Annexin V-positive) reflects the phosphatidylserine translocation to the outer surface of the plasma membrane and commitment to

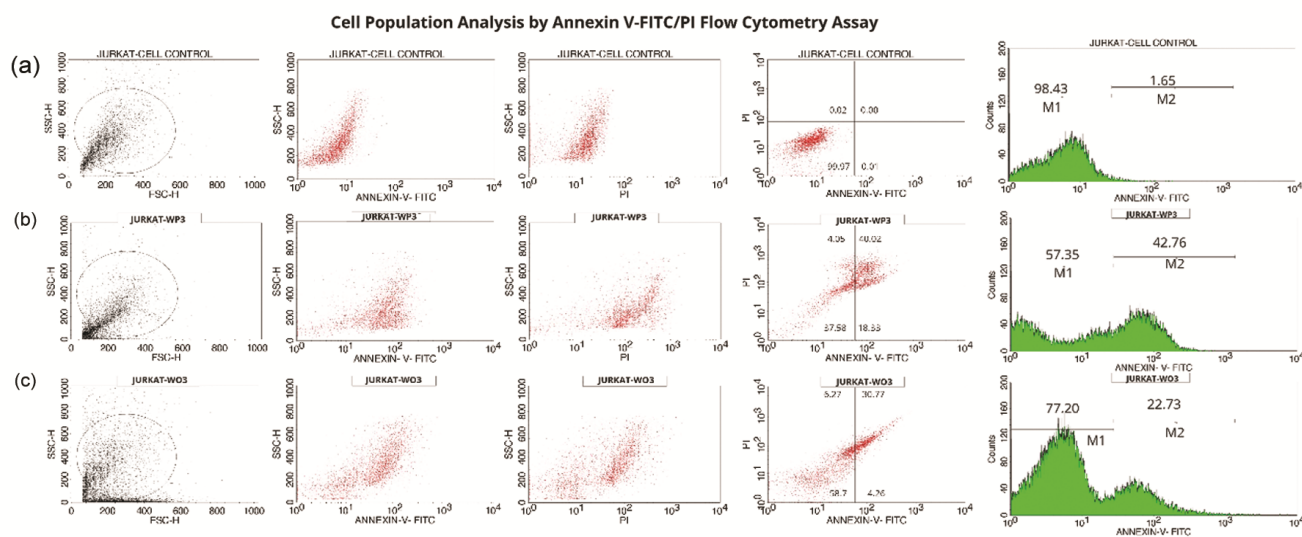


Fig. 1 — (a) cell control Quadrangular plot representing the Annexin V/PI expression in JURKAT cells upon culturing in the presence of methanolic combinatorial extracts, (b) WP3 and (c) WO3 (20 $\mu\text{g}/\text{mL}$) for 24 h and untreated control cells. The analysis was done by using BD FACS Calibur, Cell Quest Pro Software (Version: 6.0). Q1- Dead cells; Q2- Late apoptotic cells; Q3-Live cells; Q4-Early apoptotic cells. Distribution of cells shifts from M1 (Annexin V negative cells) to M2 (Annexin V positive cells)

apoptotic cell death. The redistribution of the cells from the M1 to M2 gate reflects WP3 with a more substantial apoptotic shift (M1=57.35; M2=42.76) compared with WO3 (M1=77.20; M2=22.73) showing a stronger pro-apoptotic efficacy. These results corroborated and aligned with the established bioactivity of phytoconstituents in *W. somnifera* and *P. emblica*, where withanolides and polyphenols elevate the intrinsic apoptosis, causing disruption of mitochondrial membrane potential, elevating ROS levels, and activating caspase-3^{28,29}. The higher effectiveness of WP3 suggests synergistic phytochemical interactions that amplify p53-mediated apoptotic signaling, supporting earlier work on dual-herbaltherapeutic enhancement. Supplementary Fig. S2 further supports these observations through dot-plot distribution patterns. Overall, the selective induction of apoptosis by WP3 and WO3 confirms their promise as minimally toxic phytotherapeutic candidates for hematological malignancies.

Acridineorange (AO)/ Ethidium bromide (EB) fluorescent staining

Following the apoptotic findings, AO/EB fluorescent staining further validated the induction of apoptosis by WP3 and WO3 in Jurkat E6-1 cells. WP3-treated cells showed bright green chromatin condensation, indicating early apoptosis, as observed in (Fig. 2b), while WO3 predominantly exhibited

bright orange nuclear condensation characteristic of late apoptosis (Fig. 2c). In contrast, untreated cells remained uniformly green, reflecting healthy nuclei (Fig. 2a). Minimal red-stained necrotic cells were observed, confirming that the extracts trigger programmed cell death rather than nonspecific membrane damage^{30,31}. The stronger early apoptotic signature in WP3 suggests rapid activation of mitochondrial apoptotic pathways, consistent with the reported effects of *W. somnifera*-based formulations in leukemia. These fluorescence microscopy findings align closely with Annexin V-FITC/PI flow cytometry results, reinforcing that WP3 and WO3 induce controlled apoptosis and hold strong therapeutic potential for hematological malignancies.

DNA fragmentation analysis

DNA fragmentation, a definitive marker of late-stage apoptosis, occurs through endonuclease-mediated cleavage of chromosomal DNA³². Agarose gel electrophoresis confirmed apoptotic DNA laddering in WP3- and WO3-treated Jurkat cells (20 µg/mL). Both extracts induced clear degradation of genomic DNA into internucleosomal fragments, whereas the untreated control showed intact DNA. Quantitatively, band intensities decreased from 87.97% in the control to 55.65% in WP3-treated and 37.83% in WO3-treated cells, indicating stronger late-stage apoptotic activation in WO3 as shown in (Table 1 and Fig. 3). The lane and

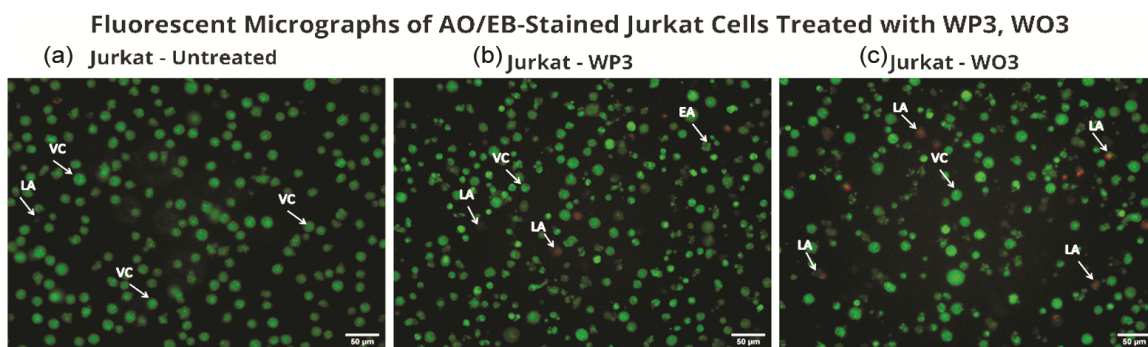


Fig. 2 — Fluorescent micrographs of Acridine Orange/Ethidium (AO/EB) double-stained Jurkat cells after 24-h incubation with methanolic combinatorial extracts WP3 and WO3 at IC₅₀ (20 µg/mL). (a) Untreated, (b) WP3-treated, (c) WO3-treated. Cells were visualized at 20× magnification. VC: Viable cells; EA: Early apoptotic cells; LA: Late apoptotic cells

Table 1 — DNA lane and band statistics calculated based on quantity regression method for evaluating the regression equation

| ID | Lane no | Band label | Base pairs (bp) | Relativ front | Adj. Vol (Int) | Volume (Int) | Absolute quantity | Relative quantity | Band % | Lane % |
|-----|---------|------------|-----------------|---------------|----------------|--------------|-------------------|-------------------|--------|--------|
| UT | 1 | 1 | 1,673 | 0.198 | 1474096 | 2298696 | 22,98,696.00 | 1 | 87.97 | 58.5 |
| UT | 1 | 2 | 933 | 0.561 | 481232 | 1338360 | 13,38,360.00 | 0.326459 | 22.18 | 12.6 |
| UT | 1 | 3 | 773 | 0.667 | 213408 | 660136 | 6,60,136.00 | 0.144772 | 9.84 | 5.6 |
| WO3 | 2 | 1 | 1,493 | 0.270 | 91879 | 385586 | 6,69,285.89 | 0.062329 | 37.83 | 13.5 |
| WO3 | 2 | 2 | 899 | 0.581 | 122181 | 499149 | 7,05,930.25 | 0.082885 | 50.31 | 18.0 |
| WO3 | 2 | 3 | 734 | 0.684 | 28773 | 366126 | 5,92,971.48 | 0.019519 | 11.84 | 4.2 |
| WP3 | 4 | 1 | 1,712 | 0.183 | 135810 | 389070 | 7,22,411.87 | 0.092131 | 55.65 | 31.9 |

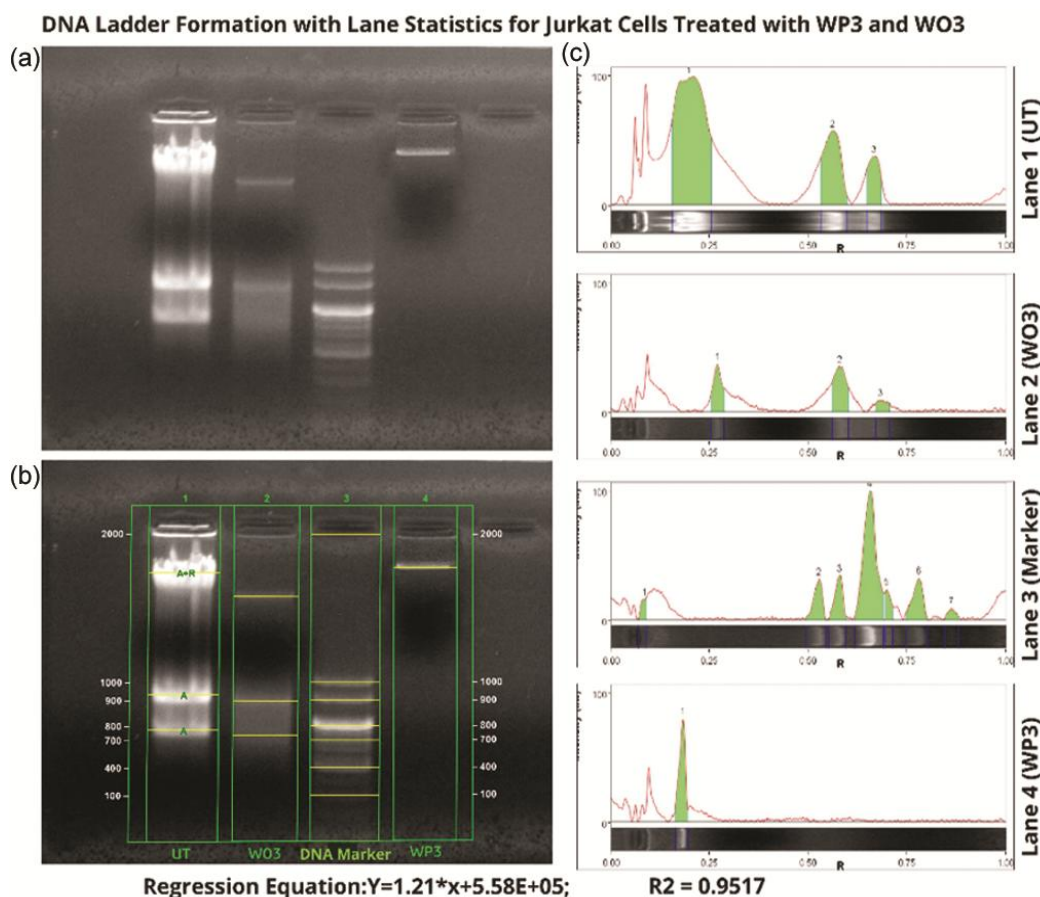


Fig. 3 — Agarose gel electrophoresis (2%) of the total DNA of Jurkat cells. From left, lane 1: Untreated control, lanes 2 and 4: WO3 (WO3) and WP3 (WP3) treated cells with 20 $\mu\text{g}/\text{mL}$ for 24 h (3 μL) and lane 3: DNA marker (1 kb). The lanes and the bands are marked to analyze the ladder formation using the Image Lab software to calculate the volume of the intensity of the bands

band analysis followed the regression model $Y = 1.21x + 5.58E+05$ ($R^2 = 0.9517$). These results support that WP3 and WO3 effectively drive cells into irreversible apoptosis, consistent with Annexin-V and AO/PI findings, confirming a controlled, synergistic apoptotic mechanism rather than nonspecific necrotic death³³⁻³⁵.

Cell cycle FACS analysis

Cell cycle disruption is a critical therapeutic approach for leukemia, as arrest at key checkpoints such as G1/S or G2/M can halt proliferation and promote apoptosis³⁶. In this study, PI-based flow cytometry was performed using WP3 and WO3 (20 $\mu\text{g}/\text{mL}$), aligned with their IC_{50} values at 24 h. Histogram analyses (Fig. 4 and Supplementary Fig. S3) treatment with WP3 and WO3 resulted in a pronounced redistribution of cells across the cell cycle phases, indicative of disrupted cell cycle progression. Both treatments reduced the G0/G1

population (54.79% and 56.82%) compared to untreated controls (69.77%), with a concomitant increase in the S-phase fraction, suggesting interference with the reported phytochemical modulation of p53 signaling and cyclin-dependent kinase pathway. The observed enrichment of the cells in the S-phase indicates disruption of DNA synthesis and replication-fork progression, a phenomenon commonly associated with activation of replication stress sensors, ATR/Chk1 signaling, and p53-mediated transcriptional responses. The S-phase arrest is consistent with previous reports showing that *Withania somnifera*-derived withanolides and *Phyllanthus emblica* polyphenols modulate cyclin-dependent kinases, suppress cyclin A/E activity, and activate p53-dependent DNA damage responses. Moreover, the marked increase in the Sub-G0/G1 hypodiploid population-WP3 (18.37%) and WO3 (6.53%) compared to the control (2.89%)-represents extensive apoptotic DNA fragmentation, confirming

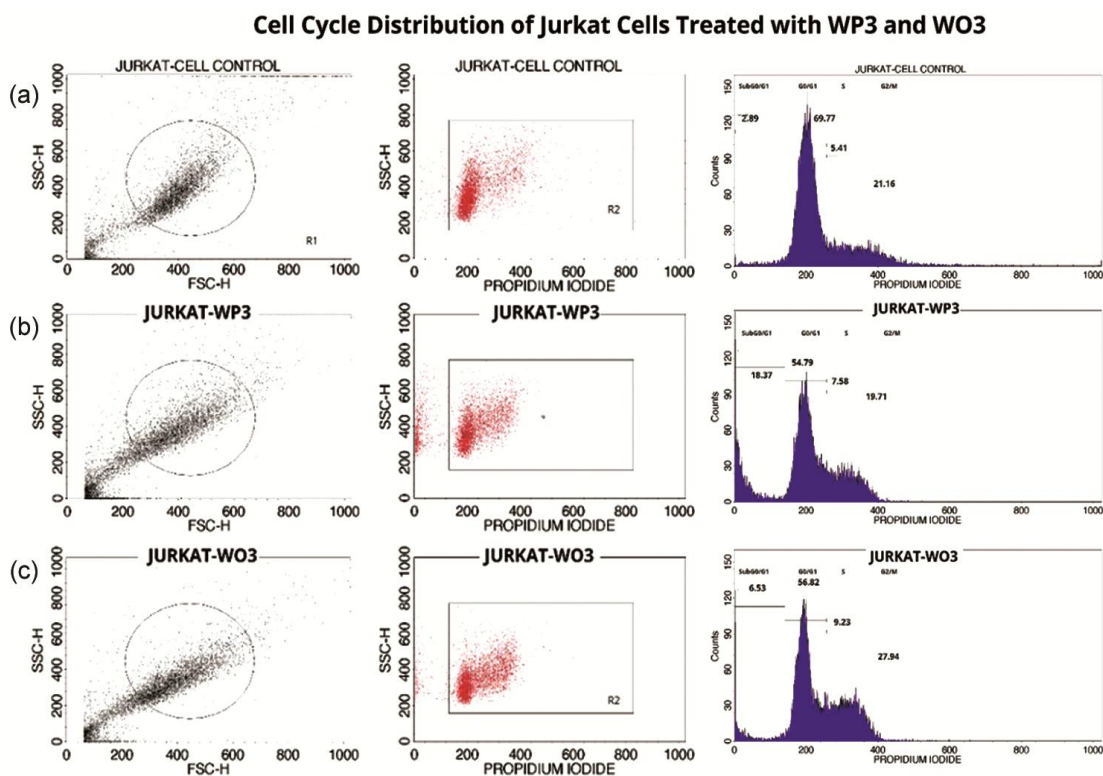


Fig. 4 — (a) Cell Cycle Analysis of Cell Control/Untreated Jurkat cells and methanolic combinatorial extract, (b) WP3 and, (c) WO3 treated after 24 h (20 $\mu\text{g/mL}$) respectively using BD FACS Calibur, BD Biosciences, CA, USA. PI histogram of the gated Cell singlets distinguishes cells at the Sub G_0/G_1 , G_0/G_1 , S, and G_2/M cycle phases. Gating of cell cycle phases is approximate and can be refined using software (Cell Quest Software, Version 6.0) analysis

that cells failing to progress past S-phase ultimately undergo programmed cell death. This is further corroborated by DNA laddering and Annexin-V results, demonstrating a coherent cascade of p53 activation, checkpoint arrest, and apoptosis. Additionally, Sub- G_0/G_1 populations increased significantly with WP3 (18.37%) and WO3 (6.53%) relative to the control (2.89%), indicating extensive apoptotic DNA fragmentation and accumulation of hypodiploid cells—consistent with the Annexin-V and DNA laddering results. These findings confirm that WP3 and WO3 inhibit leukemic cell proliferation by inducing checkpoint-mediated cell-cycle arrest, ultimately enforcing programmed cell death³⁷. Collectively, these findings indicate that WP3 and WO3 exert antiproliferative effects in Jurkat cells by disrupting cell-cycle regulation, primarily through S-phase checkpoint engagement and apoptotic commitment. The stronger response elicited by WP3 may reflect the combinatorial phytochemical interactions between *W. somnifera* and *P. emblica* that enhance DNA damage signaling and apoptotic execution pathways. Thus, both combinations

inhibit leukemic cell proliferation not merely by cytotoxicity but through precise modulation of cell-cycle checkpoints, culminating in p53-linked apoptotic cell death.

Tumor suppressor protein, p53 FACS analysis

Tumorigenesis arises from disrupted cell cycle control, resulting in uncontrolled proliferation³⁸. Cell cycle progression is regulated by cyclins, CDKs, and tumour suppressors like p53 and pRb, which safeguard genomic stability through checkpoint surveillance³⁹. Plant-derived bioactive compounds are known to modulate these regulatory pathways, leading to checkpoint arrest and apoptosis³⁷. In this study, methanolic dual herbal extracts WP3 and WO3 (20 $\mu\text{g/mL}$, 24 h) markedly increased p53 expression levels to 29.52% and 26.63%, compared to 9.04% in untreated cells, as shown in (Fig. 5 & Supplementary Fig. S4). The elevated p53 suggests activation of tumour suppressive signaling, possibly via ATM/ATR or p38/MAPK pathways, promoting checkpoint arrest at G_1/S and G_2/M and facilitating the elimination of DNA-damaged cells⁴⁰.

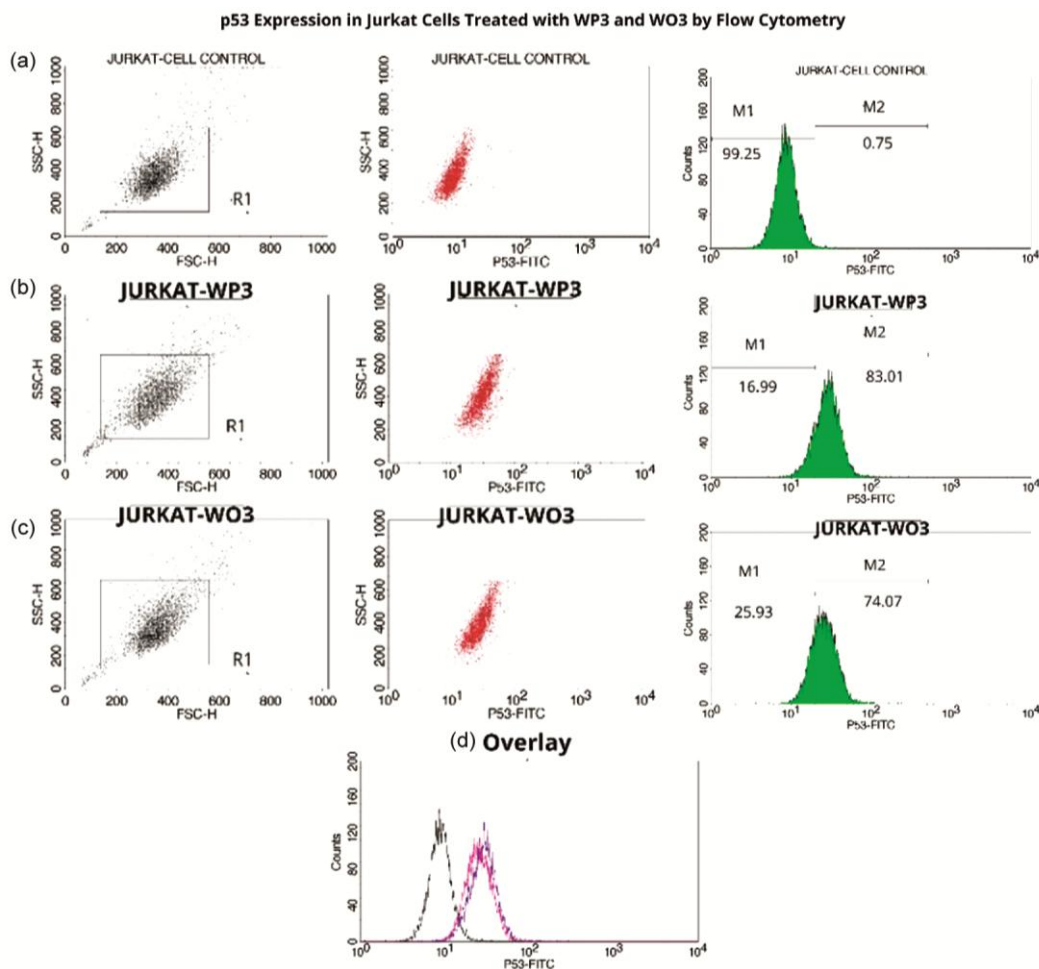


Fig. 5 — (a) Histograms depicting the p53 expression observed in untreated control, (b) WP3, and (c) WO3 treated Jurkat cell line with the incubation period of 24 h (20 $\mu\text{g}/\text{mL}$) using BD FACS Calibur, BD Biosciences, CA, USA. Histograms of the gated Jurkat singlets distinguish the cells. Overlay histogram showing blue (WP3) and rose (WO3) parameters by flow cytometry analysis. Distribution of cells shift from M1 (negative cells) to M2 (positive cells)

Conclusion

The methanolic dual-herbal combinations WP3 (*Withania somnifera* + *Phyllanthus emblica*) and WO3 (*Withania somnifera* + *Ocimum basilicum*) showed strong, selective anticancer effects on Jurkat E6-1 leukemia cells, with little toxicity to normal PBMCs—an important trait for cancer treatments. Their mechanisms of inducing apoptosis were confirmed through membrane phosphatidylserine exposure, DNA fragmentation, and chromatin condensation, along with notable disruption of the cell cycle and activation of p53-dependent checkpoints. WP3 induced a more pronounced S-phase arrest than WO3, consistent with its stronger apoptotic effects observed in Annexin V and AO/EB assays. The phytochemicals delivered cell cycle arrest and apoptotic responses by elevating the

p53 proficiency of Jurkat cells. Many hematological malignancies, including T-cell leukemia regulate on defective oncogene signals and suppression of tumor suppressor function, making p53 activation for controlling disease progression. Compared with the previous report, WP3 demonstrated greater antiproliferation activity than *P. emblica* alone, implying greater synergism between withanolides and polyphenols. Collectively, this study substantiates the scientific ayurvedic Rasayanadual herbal combinations, highlighting WP3 as a potential candidate for preclinical development in hematological malignancies. Future research studies should investigate molecular signaling cascades, *in vivo* validation, and bioactive compound-specific combinations towards translational oncology.

Supplementary Data

Supplementary data associated with this article is available in the electronic form at [https://nopr.niscpr.res.in/jinfo/ijtk/IJTK_25\(3\)\(2026\)229-238_SupplData.pdf](https://nopr.niscpr.res.in/jinfo/ijtk/IJTK_25(3)(2026)229-238_SupplData.pdf)

Author Contributions

BS: Conceptualization, methodology, software, validation, formal analysis, investigation, resources, data curation, writing-original draft. MSR: Conceptualization, Methodology, writing-original draft review and editing, visualization, Supervision.

Conflict of Interest

The authors declare no conflict of interest.

Ethics Statement

This study was conducted using commercially available established human cell lines (Jurkat E6.1 and PBMCs). As no human subjects or animal experiments were directly involved, separate ethical approval was not required. All procedures complied with institutional biosafety and ethical guidelines.

Informed Consent

Not applicable, as the study did not involve human participants, patient data, or personally identifiable information.

Data Availability

All datasets generated and analyzed during the current study are available from the corresponding author upon reasonable request. Additional supplementary data supporting the findings of this research are included within the article and its supplementary files.

References

- 1 Mallath M K, Taylor D G, Badwe R A, Rath G K, Shanta V, *et al.*, The growing burden of cancer in India: epidemiology and social context, *Lancet Oncol*, 15 (6) (2014) e205-e212. doi:10.1016/S1470-2045(14)70115-9
- 2 Stewart B W, Wild C P, World Cancer Report 2014. International Agency for Research on Cancer; 2014.
- 3 Chen L-X, He H, Qiu F, Natural withanolides: an overview, *Nat Prod Rep*, 28 (4) (2011) 705-740. doi:10.1039/c0np00045k
- 4 Vyas V K, Bhandari P & Patidar R, A comprehensive review on *Withania somnifera* dunal, *J Nat Rem*, 11 (1) (2011) 1-13. DOI: <https://doi.org/10.18311/jnr/2011/43>
- 5 Kumar P & Kumar A, Possible neuroprotective effect of *Withania somnifera* root extract against 3-nitropropionic acid-induced behavioral, biochemical, and mitochondrial dysfunction in an animal model of Huntington's disease, *J Med Food*, 12 (3) (2009) 591-600. doi:10.1089/jmf.2008.0028
- 6 Davis L & Kuttan G, Immunomodulatory activity of *Withania somnifera*, *J Ethnopharmacol*, 71 (1) (2000) 193-200. doi:10.1016/S0378-8741(99)00206-8
- 7 Rai M, Jogee P S, Agarkar G & dos Santos C A, Anticancer activities of *Withania somnifera*: Current research, formulations, and future perspectives, *Pharm Biol*, 54 (2) (2016) 189-197. doi:10.3109/13880209.2015.1027778
- 8 Zhao T, Sun Q, Marques M & Witcher M, Anticancer properties of *Phyllanthus emblica* (Indian Gooseberry), *Oxid Med Cell Longev*, 2015 (2015) 950890. doi:10.1155/2015/950890
- 9 Perna S, Alawadhi H, Riva A, Allegrini P, Petrangolini G, *et al.*, *In vitro* and *in vivo* anticancer activity of Basil (*Ocimum* spp.): current insights and future prospects, *Cancers (Basel)*, 14 (10) (2022) 2375. doi:10.3390/cancers14102375
- 10 Koczurkiewicz P, Łojewski M, Piska K, Michalik M, Wójcik-Pszczola K, *et al.*, Chemopreventive and anticancer activities of *Bacopa monnieri* extracted from artificial digestive juices, *Nat Prod Commun*, 12 (3) (2017) 337-342. doi:10.1177/1934578X1701200306
- 11 Divisha R, Ranganathan V, Vijayakaran K & Elamaram A, Evaluating *Ocimum basilicum* and *Ocimum tenuiflorum* leaf extracts for the presence of phenolic compounds, *J Pharmacogn Phytochem*, 7 (6) (2018) 2453-2456.
- 12 Kumar V, Ramamurthy P C, Singh S, Dhanjal D S, Parihar P, *et al.*, Phytochemistry and ethnomedicinal qualities of metabolites from *Phyllanthus emblica* L.: A review, *Biocell*, 47 (5) (2023) 1159-1176. doi:10.32604/biocell.2023.022065
- 13 Abraham R T & Weiss A, Jurkat T cells and development of the T-cell receptor signalling paradigm, *Nat Rev Immunol*, 4 (4) (2004) 301-308. doi:10.1038/nri1330
- 14 Basaiyye S S, Naoghare P K, Kanojiya S, Bafana A, Arrigo P, *et al.*, Molecular mechanism of apoptosis induction in Jurkat E6-1 cells by *Tribulus terrestris* alkaloids extract, *J Tradit Complement Med*, 8 (3) (2018) 410-419. doi:10.1016/j.jtcme.2017.08.014
- 15 Mahima, Rahal A, Deb R, Latheef S K, Samad H A, *et al.*, Immunomodulatory and therapeutic potentials of herbal, traditional/indigenous and ethnoveterinary medicines, *Pakistan J Biol Sci*, 15 (16) (2012) 754-774. doi:10.3923/pjbs.2012.754.774
- 16 Che C-T, Wang Z J, Chow M S S & Lam C W K, Herb-herb combination for therapeutic enhancement and advancement: theory, practice and future perspectives, *Molecules*, 18 (5) (2013) 5125-5141. doi:10.3390/molecules18055125
- 17 Bhargavi S & Shankar S R M, Dual herbal combination of *Withania somnifera* and five rasayana herbs: A phytochemical, antioxidant, and chemometric profiling, *J Ayurveda Integr Med*, 12 (2) (2021) 283-293. doi:10.1016/j.jaim.2020.10.001
- 18 Bhargavi S, Shankar S R M & Jemmy C H, *In silico* and *in vitro* studies on inhibitors for SARS-CoV-2 non-structural proteins with dual herbal combination of *Withania somnifera* with five rasayana herbs, *J Biomol Struct Dyn*, 41 (8) (2023) 3265-3280. doi:10.1080/07391102.2022.2046642

- 19 Yu D, Du Z, Li W, Chen H, Ye S, *et al.*, Targeting Jurkat T lymphocyte leukemia cells by an engineered interferon-alpha hybrid molecule, *Cell Physiol Biochem*, 42 (2) (2017) 519-529. doi:10.1159/000477601
- 20 Homburg C H, de Haas M, von dem Borne A E, Verhoeven A J, Reutelingsperger C P, *et al.*, Human neutrophils lose their surface Fc gamma RIII and acquire Annexin V binding sites during apoptosis *in vitro*, *Blood*, 85 (2) (1995) 532-540.
- 21 Rieger A M, Nelson K L, Konowalchuk J D & Barreda D R, Modified annexin V/propidium iodide apoptosis assay for accurate assessment of cell death, *J Vis Exp*, 50 (2011) 3-6. doi:10.3791/2597
- 22 Palomo I G, Jaramillo J C, Alarcon M L, Gutierrez C L, Moore-Carrasco R, *et al.*, Increased concentrations of soluble vascular cell adhesion molecule-1 and soluble CD40L in subjects with metabolic syndrome, *Mol Med Rep*, 2 (3) (2009) 481-485. doi: 10.3892/mmr_00000125
- 23 Samarghandian S & Shabestari M M, DNA fragmentation and apoptosis induced by safranal in human prostate cancer cell line, *Indian J Urol*, 29 (3) (2013) 177-183. doi:10.4103/0970-1591.117278
- 24 Reyes-Reyes E M, Jin Z, Vaisberg A J, Hammond G B & Bates P J, Physangulidine A, a withanolide from *Physalis angulata*, perturbs the cell cycle and induces cell death by apoptosis in prostate cancer cells, *J Nat Prod*, 76 (1) (2013) 2-7. doi:10.1021/np300457g
- 25 Lambkin H A, Mothersill C M & Kelehan P, Variations in immunohistochemical detection of p53 protein over expression in cervical carcinomas with different antibodies and methods of detection, *J Pathol*, 172 (1) (1994) 13-18. doi:10.1002/path.1711720105
- 26 Elmore S, Apoptosis: a review of programmed cell death, *Toxicol Pathol*, 35 (4) (2007) 495-516. doi:10.1080/01926230701320337
- 27 Habli Z, Toumeh G, Fatfat M, Rahal O N & Gali-Muhtasib H, Emerging cytotoxic alkaloids in the battle against cancer: Overview of molecular mechanisms, *Molecules*, 22 (2) (2017) 250. doi:10.3390/molecules22020250
- 28 Jung Y Y, Um J-Y, Chinnathambi A, Govindasamy C, Narula A S, *et al.*, Withanolide modulates the potential crosstalk between apoptosis and autophagy in different colorectal cancer cell lines, *Eur J Pharmacol*, 928 (2022) 175113. doi:https://doi.org/10.1016/j.ejphar.2022.175113
- 29 Gul M, Liu Z-W, Iahtisham-Ul-haq, Rabail R, Faheem F, *et al.*, Functional and nutraceutical significance of Amla (*Phyllanthus emblica* L.): A Review, *Antioxidants*, 11 (5) (2022) 816. doi:10.3390/antiox11050816
- 30 Kwan Y P, Saito T, Ibrahim D, Al-Hassan F M S, Oon C E, *et al.*, Evaluation of the cytotoxicity, cell-cycle arrest, and apoptotic induction by *Euphorbia hirta* in MCF-7 breast cancer cells, 54 (7) (2016) 1223-1236. doi: 10.3109/13880209.2015.1064451
- 31 Atteeq M, Evaluating anticancer properties of Withaferin A – a potent phytochemical, *Front Pharmacol*, 13 (2022) 975320. doi:10.3389/fphar.2022.975320
- 32 Golias C H, Charalabopoulos A & Charalabopoulos K, Cell proliferation and cell cycle control : a mini review, *Int J Clin Pract*, 58 (12) (2004) 1134-1141. doi:10.1111/j.1368-5031.2004.00284.x
- 33 Meng X, Dang T & Chai J, From Apoptosis to Necroptosis: The Death Wishes to Cancer, *Cancer Control*, 28 (2021) 10732748211066311. doi:10.1177/10732748211066311
- 34 Bhat J A, Akther T, Najar R A, Rasool F & Hamid A, *Withania somnifera* (L.) Dunal (Ashwagandha); current understanding and future prospect as a potential drug candidate, *Front Pharmacol*, 13 (2022) 1029123. doi:10.3389/fphar.2022.1029123
- 35 Crowley L C, Marfell B J, Scott A P & Waterhouse N J, Quantitation of Apoptosis and Necrosis by Annexin V binding, Propidium Iodide uptake, and flow cytometry, *Cold Spring Harb Protoc*, 2016 (11) (2016) 087288. doi:10.1101/pdb.prot087288
- 36 Cho J-H, Lee J-G, Yang Y-I, Kim J-H, Ahn J-H, *et al.*, Eupatilin, a dietary flavonoid, induces G2/M cell cycle arrest in human endometrial cancer cells, *Food Chem Toxicol*, 49 (8) (2011) 1737-1744. doi:https://doi.org/10.1016/j.fct.2011.04.019
- 37 Ahmad S S, Garg C, Bhat A H & Kaur S, Phytochemicals in cancer therapy: modulating cell cycle, angiogenesis, and epithelial-mesenchymal transition, *Revista Brasileira de Farmacognosia*, 35 (2) (2025) 255-274. doi:10.1007/s43450-025-00620-4
- 38 Zhang W-K, Xu J-K, Zhang X-Q, Yao X-S & Ye W-C, Chemical constituents with antibacterial activity from *Euphorbia sororia*, *Nat Prod Res*, 22 (4) (2008) 353-359. doi:10.1080/14786410701838114
- 39 Zhu D-M, Xue W-L, Tao W & Li J-C, Biological effects of ray cartilage extract on human breast cancer cell line MCF-7 and its mechanism, *Int J Clin Exp Med*, 8 (5) (2015) 7425-7429.
- 40 Ozaki T & Nakagawara A, Role of p53 in cell death and human cancers, *Cancers (Basel)*, 3 (1) (2011) 994-1013. doi: 10.3390/cancers3010994